



Mitochondrial AAA-ATPase Msp1 detects mislocalized tail-anchored proteins through a dual-recognition mechanism

Lanlan Li^{1,2,3,‡}, Jing Zheng^{2,3,4,‡}, Xi Wu^{2,†,*}  & Hui Jiang^{2,3,5,**} 

Abstract

The conserved AAA-ATPase Msp1 is embedded in the outer mitochondrial membrane and removes mislocalized tail-anchored (TA) proteins upon dysfunction of the guided entry of tail-anchored (GET) pathway. It remains unclear how Msp1 recognizes its substrates. Here, we extensively characterize Msp1 and its substrates, including the mitochondrially targeted Pex15 Δ 30, and full-length Pex15, which mislocalizes to mitochondria upon dysfunction of Pex19 but not the GET pathway. Moreover, we identify two new substrates, Frt1 and Ysy6. Our results suggest that mislocalized TA proteins expose hydrophobic surfaces in the cytoplasm and are recognized by Msp1 through conserved hydrophobic residues. Introducing a hydrophobic patch into mitochondrial TA proteins transforms them into Msp1 substrates. In addition, Pex15 Δ 30 and Frt1 contain basic inter-membrane space (IMS) residues critical for their mitochondrial mistargeting. Remarkably, Msp1 recognizes this feature through the acidic D12 residue in its IMS domain. This dual-recognition mechanism involving interactions at the cytoplasmic and IMS domains of Msp1 and substrates greatly facilitates substrate recognition and is required by Msp1 to safeguard mitochondrial functions.

Keywords AAA+ ATPase; ATAD1; mitochondrial protein quality control; Msp1; tail-anchored proteins

Subject Categories Membrane & Intracellular Transport; Protein Biosynthesis & Quality Control

DOI 10.15252/embr.201846989 | Received 31 August 2018 | Revised 28 January 2019 | Accepted 11 February 2019 | Published online 11 March 2019

EMBO Reports (2019) 20: e46989

Introduction

Mitochondria are essential organelles that play pivotal roles in energy supply, metabolism, and signaling processes such as cell

death. Mitochondrial proteostasis is critical for mitochondrial fitness and is maintained by AAA-proteases [1,2], the ubiquitin-Cdc48-proteasome pathway [3–5], and an AAA-ATPase Msp1 embedded in outer mitochondrial membrane (OMM) that clears mislocalized tail-anchored (TA) proteins [6,7].

TA proteins are post-translationally targeted to the ER, peroxisome, and mitochondria [8]. The best understood TA protein targeting pathway is the guided entry of tail-anchored (GET) pathway: Newly synthesized TA protein is recognized at the transmembrane (TM) segment by the chaperone Sgt2, then delivered to the ATPase Get3, and finally transferred to the Get1/2 insertase complex at ER membrane [9,10]. In *get* mutant cells, many GET-dependent TA proteins accumulate as aggregates in the cytoplasm, and a subset of them are mistargeted to mitochondria [11]. OMM contains important TA proteins, including the fission receptor Fis1 [12], the ER-mitochondria encounter structure component Gem1 [13], and subunits of the TOM import complex including Tom5, Tom6, Tom7, and Tom22 [14]. It remains unclear that how TA proteins are targeted to mitochondria as none of the known mitochondrial import machineries is required for their biogenesis [15,16].

Msp1 is an evolutionarily conserved AAA-ATPase (ATAD1 in human) that dually localizes to mitochondria and peroxisome. It removes TA proteins mistargeted to mitochondria in *get* mutant cells to safeguard mitochondrial function. Synthetic mutations of *MSP1* and GET genes cause the accumulation of mistargeted TA proteins on mitochondria, resulting in severe mitochondrial defects and poor respiratory growth [6,7]. Peroxisomal Msp1 clears excessive TA protein Pex15 that fails to assemble into complex with its binding partner Pex3 [17]. ATAD1 knockout mice and patients carry ATAD1 mutations show severe mitochondrial damages [6,18]. It is interesting and essential to understand how Msp1 detects and distinguishes its substrates from mitochondrial TA proteins.

Msp1 belongs to the meiotic clade of AAA proteins that contains an N-domain followed by an AAA-ATPase domain [19]. Other members of this clade include Vps4, Spastin, Katanin, and Fidgetin.

1 College of Life Sciences, Beijing Normal University, Beijing, China

2 National Institute of Biological Sciences, Beijing, China

3 Beijing Key Laboratory of Cell Biology for Animal Aging, Beijing, China

4 School of Life Sciences, Peking University, Beijing, China

5 Tsinghua Institute of Multidisciplinary Biomedical Research, Tsinghua University, Beijing, China

*Corresponding author. Tel: +86 10 58958215; E-mail: xi.wu@beigene.com

**Corresponding author. Tel: +86 10 80723279; E-mail: jianghui@nibs.ac.cn

‡These authors contributed equally to this work

†Present address: BeiGene, Beijing, China

Studies of these four enzymes suggest common features that they exist as monomers/dimers, directly bind substrates through the N-terminal microtubule interacting and trafficking (MIT) domain, and assemble into hexamer upon substrate engagement [20]. Msp1 alone is sufficient to dislocate TA protein from liposome as shown in an *in vitro* assay [21], indicating Msp1 can directly recognize substrates. But as the only transmembrane protein in this clade, Msp1 possesses a different N-domain that contains a TM segment and lacks homology to those of other members [19]. Furthermore, epichromosomally expressed Msp1 N-domain mutants can rescue *msp1Δ* cells [21], arguing against a role of Msp1 N-domain in substrate recognition. Msp1 also interacts with Cis1, a stress-responsive protein that facilitates the Msp1-dependent removal of mitochondrial precursor proteins clogged in the TOM complex [22]. Whether Cis1 is involved in the removal of mistargeted TA proteins remains unclear. In this study, we combine genetic, biochemical, and imaging approaches to address the molecular mechanisms of substrate recognition by Msp1.

Results

Identification of Msp1 N-domain residues critical for GFP-Pex15Δ30 binding

Msp1 function was determined by monitoring the degradation of its model substrate GFP-Pex15Δ30, in which the last 30 amino acids of Pex15 were truncated to make it constitutively targeted to mitochondria [7]. Cis1 knockout did not affect GFP-Pex15Δ30 degradation (Appendix Fig S1). We thus focused on Msp1 itself. Msp1 consists of an N-domain of 98 amino acids, and a C-terminal AAA-domain highly analogous to other AAA-ATPases (Fig 1A). We rescued *msp1Δ* cells with wild-type (WT) Msp1 or Msp1^{TOM70(N)}, in which the N-terminal 32 residues of Msp1 were replaced with those of Tom70 (Fig EV1A). When expressed by epichromosomal vector under the control of Msp1 promoter, Msp1^{TOM70(N)} restored GFP-Pex15Δ30 degradation and rescued the growth defect of *get3Δ msp1Δ* cells under respiratory growth condition (SCEG; Fig EV1B and C), consistent with previous results [21]. In contrast, when expressed by knockin, Msp1^{Tom70(N)} did not rescue these defects

(Fig EV1B and C). Epichromosomal expression produced three times more proteins than the knockin method (Fig EV1D), suggesting that Msp1 N-domain contains key residues facilitating substrate degradation, and the loss of these residues requires compensation by Msp1 overexpression. Furthermore, epichromosomal expression resulted in heterogeneous expression (Fig EV1E). We thus utilized the knockin method to analyze Msp1 N-domain mutants.

Alignment of the N-domain sequences of Msp1 and its orthologs revealed conserved residues (Fig 1A). We performed mutagenesis scan of 39 residues within and flanking the TM domain and in the conserved C-terminal region (marked by asterisks in Fig 1A). The L122, 123D mutant disrupts Msp1 hexamer assembly [21] and thus served as a control for Msp1 loss of function. We identified 11 residues whose mutations did not affect Msp1 localization (Fig EV2A) and stability (Fig 1B) but impaired GFP-Pex15Δ30 degradation (Figs 1B and EV2B). The untagged Msp1 V81A and I93A mutants also impaired substrate degradation (Fig EV2C). We further examined whether Msp1 stability and folding were affected by the mutants. The thermostability of endogenous Msp1 was not affected by V81A and I93A mutations (Appendix Fig S2A–D). We then generated recombinant proteins of Msp1 cytoplasmic domain. WT Msp1 and its V81A, I86A, I93A, and G95A mutants had similar sensitivity to limited trypsin digestion (Appendix Fig S2E). These results indicate the N-domain mutants did not alter Msp1 structure. These residues are highlighted in red (Fig 1A) and most of them are evolutionarily conserved. Notably, D12 is lost in the Msp1^{TOM70(N)} mutant.

The E193Q walker B mutant of Msp1 has normal ATP binding but loses ATP hydrolysis activity. It forms a hexamer and constitutively binds substrates and thus functions as a substrate-trap mutant [6,7,21]. When assayed by blue-native gel, Msp1-FLAG existed as monomers and Msp1^{E193Q}-FLAG as hexamers (Fig 1C, lanes 2 and 3), a typical feature of meiotic clade of AAA-ATPases [20]. Msp1^{L122,123D,E193Q} served as a control to disrupt hexamer assembly. Most mutations did not affect the oligomerization of Msp1^{E193Q}-FLAG except Y72A, which caused a slight increase of monomeric forms (Fig 1C, lane 7). We then analyzed substrate binding with Msp1. As expected, Msp1^{E193Q}-FLAG pulled down GFP-Pex15Δ30, whereas Msp1-FLAG did not (Fig 1D, lanes 2 and 3). Nearly, all the mutations except G94A impaired GFP-Pex15Δ30 pulldown by

Figure 1. Identification of residues in Msp1 N-domain essential for GFP-Pex15Δ30 binding.

- Alignment of Msp1 N-domain sequence (amino acids 1–98) with those of its orthologs. Residues marked by asterisks were tested for their roles in GFP-Pex15Δ30 degradation. The critical residues are highlighted in red.
- Degradation of GFP-Pex15Δ30 in strains expressing WT or mutant forms of Msp1-FLAG. Cells were grown in synthetic glucose media (SCD) to log phase, treated with cycloheximide (CHX) to stop protein synthesis, and collected at the indicated time points. L122, 123D mutation disrupts Msp1 hexamer assembly and thus served as a control for Msp1 loss of function. Anti-Por1 blots were shown as the loading controls.
- Hexamer assembly by WT and mutant forms of Msp1-FLAG. Mitochondria-enriched fraction was isolated from the indicated knockin strains, lysed with 1% digitonin. Lysates (10 μg) were analyzed by blue-native (BN) PAGE or SDS–PAGE.
- Interaction of GFP-Pex15Δ30 with WT and mutant forms of Msp1-FLAG. Mitochondria were isolated, lysed with 1% digitonin, and subject to anti-FLAG immunoprecipitation (IP). Mitochondrial extracts (10 μg) and immunoprecipitates (100 μl in total, load 1 μl for FLAG and 10 μl for GFP blot) were analyzed by Western blot. The intensity ratio of GFP-Pex15Δ30/Msp1-FLAG was calculated using ImageJ software and normalized to the value of positive control (GFP-Pex15Δ30/Msp1^{E193Q}-FLAG).
- The positions of conserved critical residues for substrate binding in the monomeric (PDB ID: 5W0T) and hexameric structures of Msp1 [21]. Three subunits of the hexamer were removed to visualize pore loop 1 (yellow). The AAA-domain is in light gray and part of the N-domain (amino acids 58–98) is in light green. Critical residues are highlighted in red. OMM: outer mitochondrial membrane.

Data information: In this figure, GFP-Pex15Δ30 was expressed from a centromeric plasmid under the control of *TEF1* promoter, and WT and mutant forms of Msp1-FLAG were expressed from the endogenous chromosomal locus.

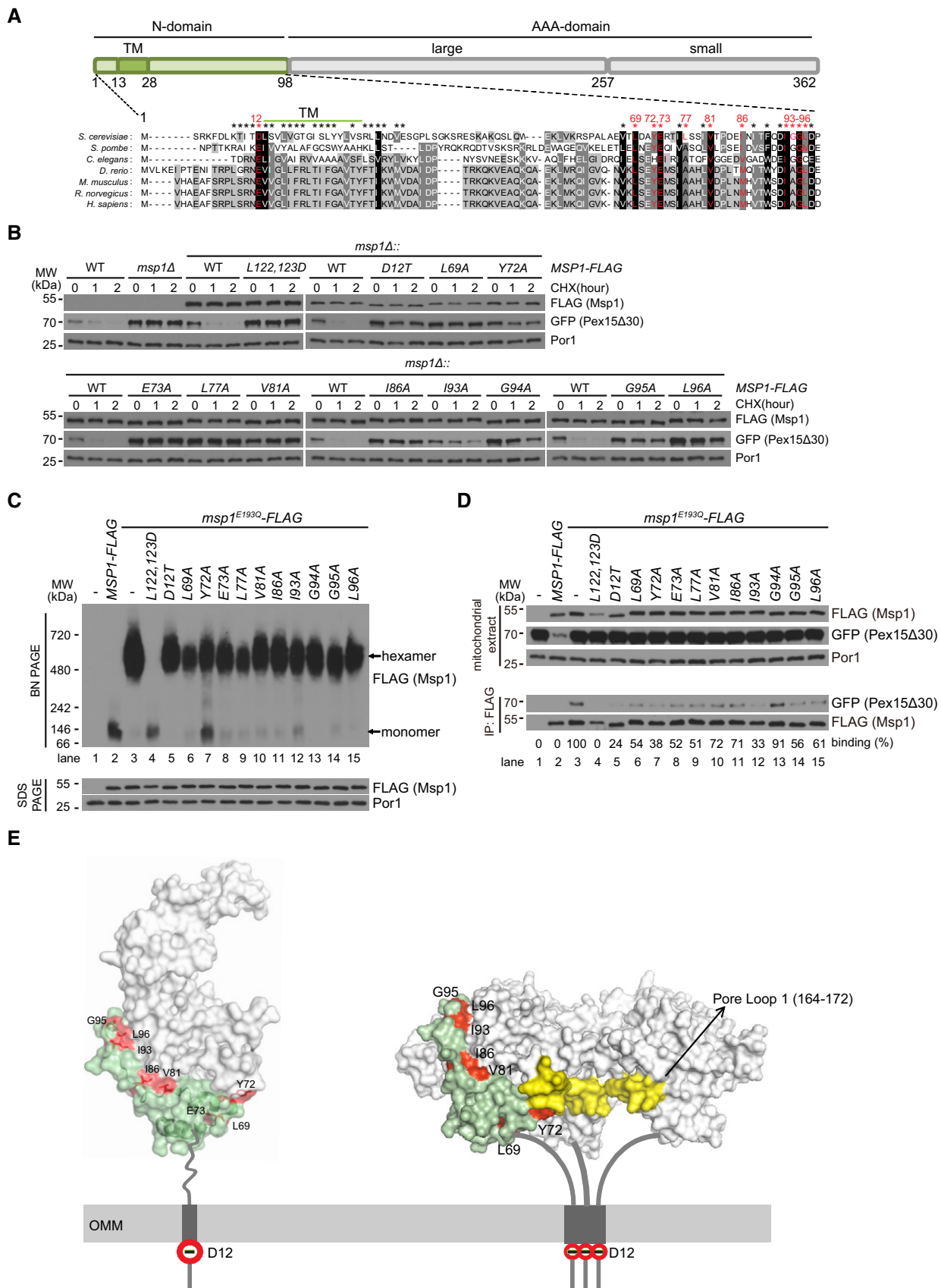


Figure 1.

Msp1^{E193Q}-FLAG (Fig 1D, lanes 5–15). Therefore, most of the residues are required for substrate binding.

We highlighted all the conserved residues critical for substrate binding on Msp1 monomeric (PDB ID: 5W0T) and hexameric structures [21] (Fig 1E): D12 is a negatively charged residue in the intermembrane space (IMS) and the other residues are in the cytoplasm. Notably, most cytoplasmic critical residues are in the folded region and are hydrophobic residues, except E73 and G95. Y72, V81, I86, I93, and L96 are in contact with the AAA-domain (light gray), most possibly to avoid exposing hydrophobic surfaces to the cytoplasm. Hydrophobic residues L69 and Y72, especially the latter, are close to pore loop 1, which is critical for substrate translocation into the pore [21].

Characterization of Msp1 and GFP-Pex15Δ30 interaction by *in vivo* site-specific photo-crosslinking

Msp1 N-domain may interact with substrates through the IMS and cytoplasmic regions because critical residues are present in both regions. We thus characterized the interaction between Msp1^{E193Q}-FLAG and GFP-3xHA-Pex15Δ30 by the *in vivo* site-specific photo-crosslinking method [23,24]. Photo-activatable amino acid *p*-benzoyl-L-phenylalanine (BPA) was introduced at a position specified by an amber codon in the target protein. Upon UV irradiation of living cells, BPA photo-crosslinks with direct interacting proteins. By sampling multiple positions, the interaction surface consisting of residues positive for BPA photo-crosslinking can be mapped. We and others have utilized the method to characterize mitochondrial complexes [25–27].

Substrate-trap mutants of AAA-ATPase can engage substrates into the central pore formed by the ATPase hexamer [28], which contains three conserved pore loops critical for substrate translocation (Fig 2A) [21]. BPA incorporated at Msp1^{E193Q} pore loops crosslinked with GFP-3xHA-Pex15Δ30 (Fig 2B, crosslinked residues are color-labeled in Fig 2A), indicating Msp1 AAA-domain works in a similar manner as other AAA-ATPases.

We then incorporated BPA into Msp1^{E193Q} N-domain (Fig 2C). We excluded most critical residues of Msp1 N-domain from BPA incorporation because incorporating BPA into these residue positions is similar to alanine mutation and may disrupt substrate interaction and cause false-negative results. We also incorporated BPA into residues 260–352 of Pex15Δ30 (Fig 2D), which contains all the critical elements for recognition by Msp1 (see Fig 3 for evidence). As summarized in Fig 2E, two features and indications can be obtained: (i) Direct interaction between Msp1 N-domain and Pex15Δ30 extensively occurs in their IMS, TM, and cytoplasmic regions. (ii) The folded region of Msp1 N-domain (amino acids 50–98, shown in green in the structural models) lines along the surface of Msp1 hexamer to positions near pore loop 1 and has direct interactions with Pex15Δ30 (crosslinked residues shown in red in the structural models). This spatial organization may facilitate substrate transfer from N-domain into the central pore.

Positively charged residues in IMS tail of GFP-Pex15Δ30 correlate with its recognition and removal by Msp1

The negatively charged D12 residue of Msp1 is critical for substrate binding (Fig 1D). Msp1 D12E mutation did not affect,

whereas D12A and D12K mutations impaired substrate degradation (Fig 3A), indicating the negative charge of D12 is critical for its function. D12 may interact with the IMS tail of substrates through electrostatic interactions considering the presence of three positively charged K residues in Pex15Δ30 IMS tail (Fig 3B). We mutate these K residues, but even mutating one K to H mistargeted GFP-Pex15Δ30 to the cytoplasm (Fig EV3A). This result is consistent with previous observations that positively charged residues in IMS tail are critical for the mitochondrial targeting of many TA proteins [8,29,30].

Outer mitochondrial membrane TA proteins Tom5, Gem1, and Fis1 carry IMS sequences rich in positively charged residues, but Tom6 does not (Fig 3B). We thus replaced the OMM targeting sequence (OTS) of GFP-Pex15Δ30 with that of OMM TA proteins. The chimeric proteins correctly localized to mitochondria (Fig EV3B). OTSs with positively charged residues (Tom5, Gem1, and Fis1) supported the degradation of chimeric proteins by Msp1 (Fig 3C). Similar to GFP-Pex15Δ30, the degradation was impaired by the Msp1^{D12T} mutation (Fig 3C). In contrast, the chimeric protein with Tom6 OTS was stable (Fig 3C). Consistent with the degradation results, OTSs of Tom5, Gem1, and Fis1 but not Tom6 supported substrate interaction with Msp1 (Fig 3D). We also tried to reduce positive charges in Tom5, Gem1, and Fis1 IMS tails. But again all the mutants tested were mislocalized (Fig EV3A). Taken together, these results support the idea that positively charged residues in substrate IMS tail facilitate their interaction with Msp1, very likely through electrostatic interactions with Msp1 D12 residue.

A hydrophobic patch in GFP-Pex15Δ30 cytoplasmic domain is essential for its recognition and removal by Msp1

The enrichment of hydrophobic critical residues in Msp1 N-domain suggests hydrophobic interactions might occur between Msp1 and substrate cytoplasmic domains. Hydrophobicity analysis revealed a hydrophobic patch near Pex15 TM segment (Fig 3E). The hydrophobic patch is rich in residue positions showing crosslinking with Msp1 (Fig 2E). Serial truncations showed that a minimum sequence (Δ1–311) consisting of the hydrophobic patch, TM segment, and IMS tail is sufficient for interaction with and removal by Msp1 (Fig 3F and G). Further deletion of the hydrophobic patch (Δ1–324) rendered the protein stable and unrecognized by Msp1 (Fig 3F and G). Deleting the hydrophobic patch alone (Δpatch) abolished the interaction between GFP-Pex15Δ30 and Msp1 (Fig 3G), and caused GFP-Pex15Δ30 degradation by an Msp1-independent mechanism (Fig 3F). All the GFP-Pex15Δ30 truncation mutants correctly localized to mitochondria (Fig EV3C). These results demonstrate that the hydrophobic patch of GFP-Pex15Δ30 is essential for its recognition and removal by Msp1.

In the patch, I313, F320, and L324 likely form a hydrophobic core, with potential contribution from flanking L316 and A317 (Fig 4A). To determine whether this hydrophobic core is required for GFP-Pex15Δ30 recognition by Msp1, we mutated three residues into non-hydrophobic ones (I313S, F320S, and L324G). Surprisingly, this mutant form mislocalized to the cytoplasm (Fig EV3D), suggesting hydrophobic residues in the patch are critical for mitochondrial targeting. We then mutated these residues to A (Fig 4B, mut1), which is of medium hydrophobicity and correctly localized to

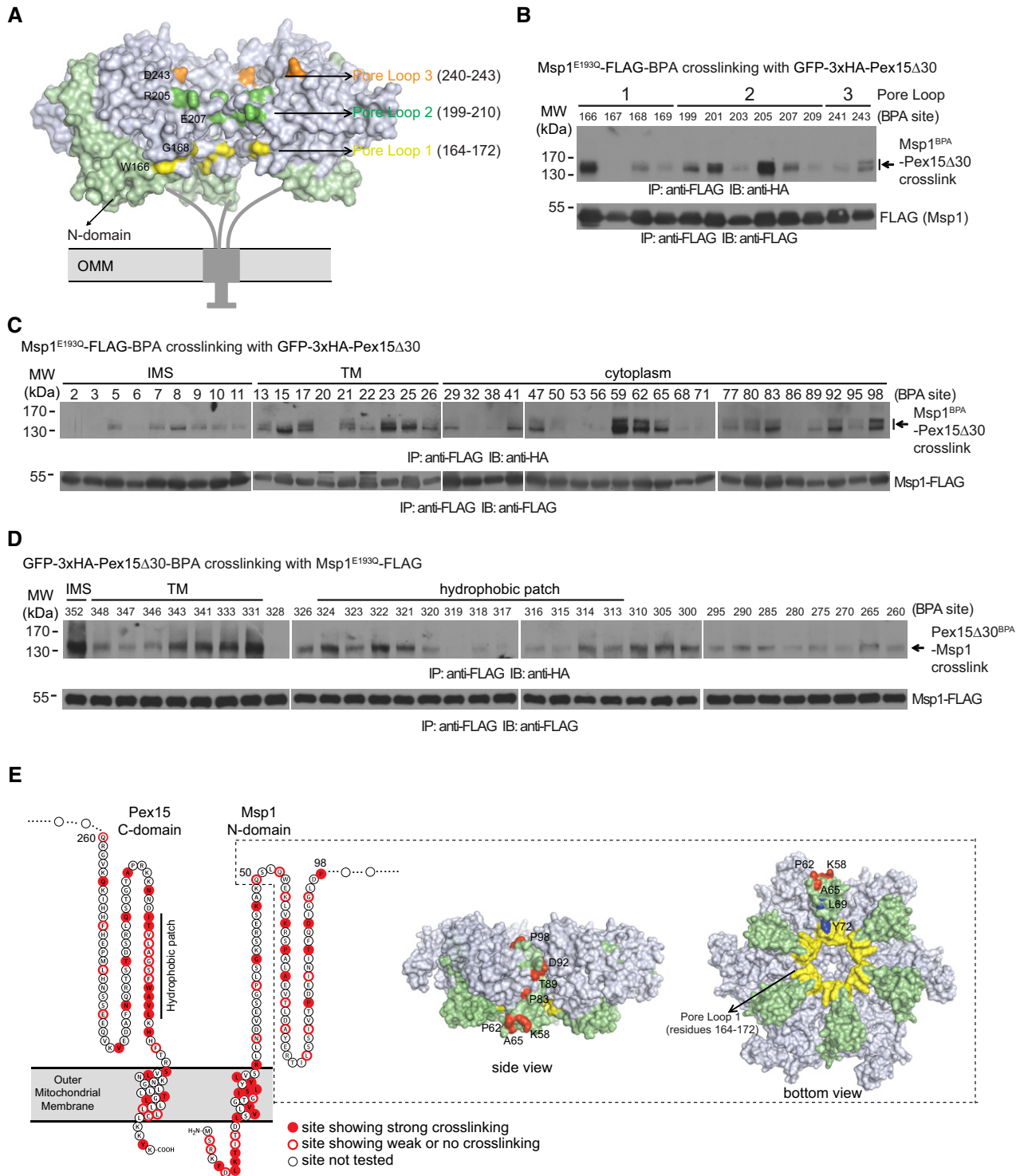


Figure 2. Characterization of GFP-3xHA-Pex15Δ30 and Msp1^{E193Q}-FLAG interaction by *in vivo* site-specific photo-crosslinking.

A A hexameric model of Msp1 with pore loop residues positive for crosslinking highlighted by colors.
B, C *In vivo* photo-crosslinking of BPA incorporated in pore loops (B) and N-domain (C) of Msp1^{E193Q}-FLAG with GFP-3xHA-Pex15Δ30.
D *In vivo* photo-crosslinking of BPA incorporated in GFP-3xHA-Pex15Δ30 (amino acids 260–352) with Msp1^{E193Q}-FLAG. Experiments in (B–D) were performed as described in Materials and Methods. Immunoprecipitates (100 μl in total, load 1 μl for FLAG, and 40–50 μl for HA blot) were analyzed by Western blot. IMS, intermembrane space.
E Cartoon summary of photo-crosslinking results. The sites showing strong (filled red) and weak or no (red circle) crosslinking are highlighted in the topology model. The boxed region highlights the position of N-domain (amino acids 50–98, shown in green) in the hexameric model of Msp1. N-domain residues positive for crosslinking (red), hydrophobic residues (L69 and Y72, blue) critical for substrate binding, and pore loop 1 (yellow) are highlighted.

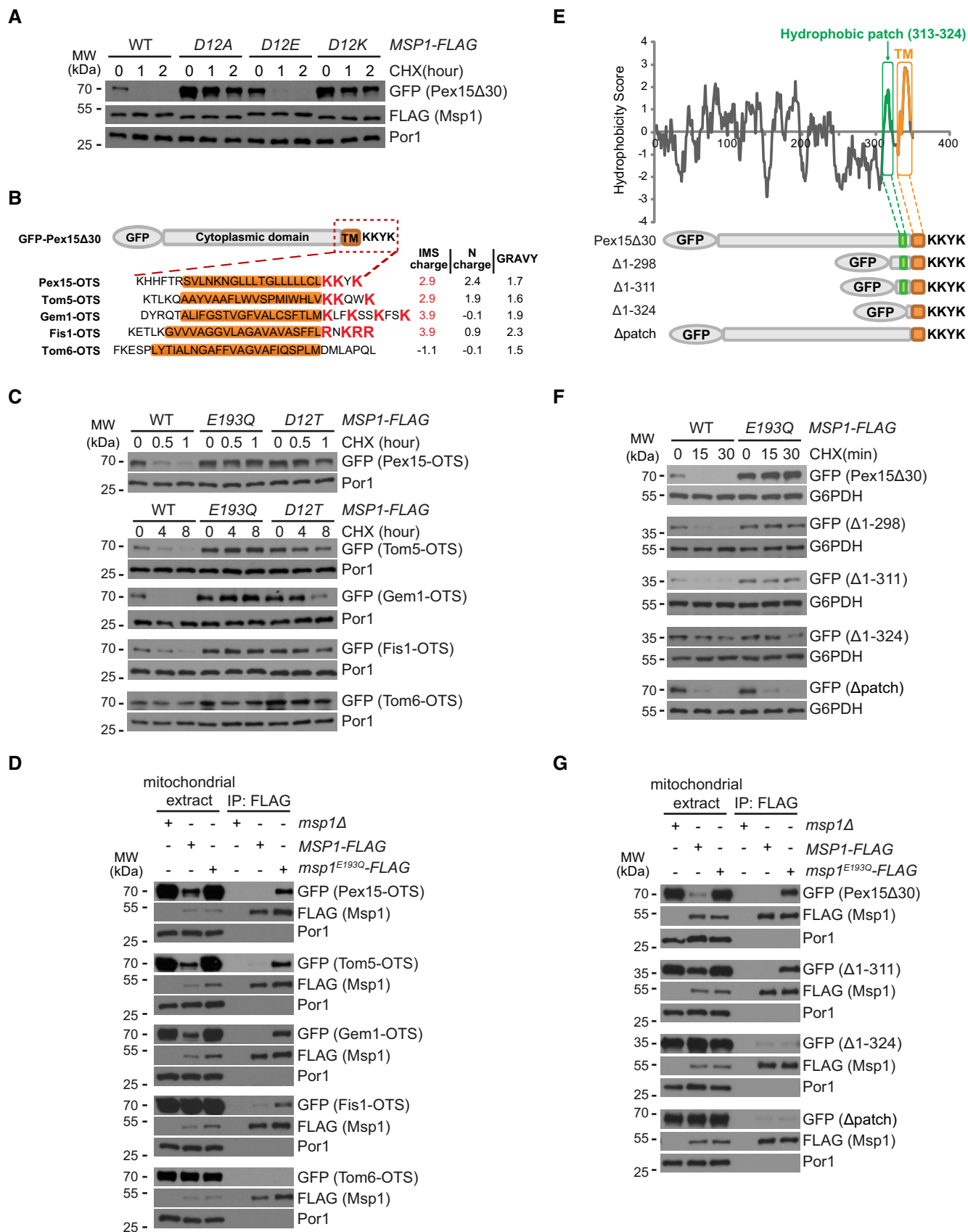


Figure 3.

Figure 3. The IMS tail charge and cytoplasmic hydrophobic patch of Pex15Δ30 are required for its recognition and removal by Msp1.

- A Degradation of GFP-Pex15Δ30 by Msp1 D12 mutants.
 B Schematic illustration of the Outer mitochondrial membrane Targeting Sequences (OTSS) of GFP-Pex15Δ30 and mitochondrial TA proteins. The GRAVY (Grand Average of Hydropathicity) values of TM domain (highlighted in orange) and the charges of the flanking sequences are shown on the right.
 C Degradation of GFP-Pex15Δ30 and its chimeric variants by Msp1.
 D Interaction of GFP-Pex15Δ30 and its chimeric variants with Msp1. Experiments were performed as in Fig 1D.
 E Hydrophobicity plot of Pex15Δ30 using the Kyte–Doolittle scale. The hydrophobic patch and the TM domain are highlighted in green and orange, respectively. Truncated forms of Pex15Δ30 are shown below.
 F Degradation of GFP-Pex15Δ30 and its truncation mutants.
 G Interaction of GFP-Pex15Δ30 and its truncation mutants with Msp1. Cells were analyzed as in (D).

Data information: In this figure, GFP-Pex15Δ30 and its mutants were expressed from a centromeric plasmid under the control of *TEF1* promoter, and WT and mutant forms of Msp1-FLAG were expressed from the endogenous chromosomal locus.

mitochondria (Fig EV3D). GFP-Pex15Δ30-mut1 degradation was partially delayed in *msp1^{E193Q}* cells and mainly degraded by an Msp1-independent mechanism (Fig 4B), similar as the degradation of the Δpatch mutant (Fig 3F). We screened a panel of mutants and found that temperature-sensitive inactivation of the ATPase subunits of proteasome Cim3 delayed GFP-Pex15Δ30-mut1 degradation. Inactivating Cim3 in *msp1Δ* cells efficiently blocked GFP-Pex15Δ30-mut1 degradation (Fig 4C). GFP-Pex15Δ30-mut1 accumulated on mitochondria in Msp1 and Cim3 mutant strains (Fig 4D), allowing us to examine its interaction with Msp1. In comparison with GFP-Pex15Δ30, GFP-Pex15Δ30-mut1 had significantly weaker interaction with Msp1^{E193Q}-FLAG (Fig 4E, lane 3 vs. 6) and the weak interaction was not enhanced by inactivating Cim3 (Fig 4E, lane 6 vs. 9). Collectively, these results suggest that the hydrophobic core in the patch of GFP-Pex15Δ30 is crucial for its recognition by Msp1.

Insertion of the hydrophobic patch into OMM TA proteins transforms them into Msp1 substrates

The OMM TA proteins Gem1 and Fis1 contain positively charged IMS residues but are not degraded by Msp1. A possible reason is that these authentic OMM TA proteins do not expose hydrophobic surfaces in their cytoplasmic domains to be recognized by Msp1. We thus introduced the hydrophobic patch into these proteins. GFP-Gem1 is stable in WT cells, but inserting the hydrophobic patch right before its OTS caused Gem1 degradation by Msp1 (GFP-Gem1-patch in Fig 4F). Patches with reduced hydrophobicity (mut2 and mut3) could not transform Gem1 into Msp1 substrate (Fig 4F). Consistently, Gem1 with WT but not mutant hydrophobic patch interacted with Msp1 (Fig 4G). Similarly, inserting the hydrophobic patch but not its mutant form (mut4) right before Fis1 OTS turned Fis1 into Msp1 substrate (Fig 4H). All the Gem1 and Fis1 mutants correctly localized to mitochondria (Fig EV3E and F). Msp1 N-domain is close to membrane, which may impose spatial constraints on substrate recognition. Hydrophobic patch inserted at the N-terminus of GFP (patch-GFP-Fis1) could not convert Fis1 into Msp1 substrate (Fig 4H), suggesting the existence of spatial constraints.

Pex15 is mistargeted to mitochondria and removed by Msp1 in *pex19Δ* cells

We then examined the turnover of full-length GFP-Pex15. The reported GET substrates (Pex15, Gos1, and Ubc6) that mislocalize to mitochondria in *get* mutant cells were identified by overexpression

[6,7,11]. Epichromosomal overexpression of GFP-Pex15 under the control of *TEF1* promoter did partially accumulate on mitochondria in *get3Δ*, *msp1Δ*, and *get3Δ msp1Δ* cells (Fig EV4). However, when chromosomally expressed by its promoter, GFP-Pex15 did not localize to mitochondria (Fig 5A) but remained peroxisomal (Fig 5B). Pex19 binds the TM segment of peroxisomal TM proteins and targets them to peroxisome [31–35]. GFP-Pex15 disappeared in *pex19Δ* cells (Fig 5C), indicating Pex15 is mistargeted and degraded. Mitochondrial accumulation of GFP-Pex15 was detected in part of *pex19Δ msp1Δ* cells (~ 32%), and greatly enhanced in *pex19Δ get3Δ msp1Δ* cells (~ 86%; Fig 5C and D). These results suggest that Pex19 mediates the sorting of endogenous Pex15. Pex15 is likely mistargeted to both the ER and mitochondria in *pex19Δ* cells, and mostly to mitochondria in *pex19Δ get3Δ* cells. Msp1 knockout saves mitochondrial Pex15. We then rescued *pex19Δ msp1Δ* and *pex19Δ get3Δ msp1Δ* cells with Msp1 N-domain mutants. The hydrophobic residues are required for removing GFP-Pex15, but D12 is largely not required (Fig 5D). These results indicate that Msp1 hydrophobic residues and D12 play key and facilitatory roles in substrate recognition, respectively. The facilitatory role of D12 is no longer rate-limiting when substrates are expressed at low level (chromosomally expression by endogenous promoter) or when Msp1 mutant without D12 is overexpressed (Fig EV1B and C).

Knocking out *PEX19* did not affect cell growth in WT, *msp1Δ*, and *get3Δ* cells, but aggravated the growth defect of *get3Δ msp1Δ* cells under fermentable growth condition (SCD; Fig 5E), suggesting the mislocalization of Pex19 substrates to mitochondria contributes to mitochondrial dysfunction.

Identification of Msp1 substrates mistargeted to mitochondria upon dysfunction of the GET pathway

Similar as Pex15, when GFP-tagged Gos1 and Ubc6 were expressed at near physiological level, they weakly mislocalized to mitochondria in *get3Δ* and *get3Δ msp1Δ* cells (< 5%; Fig 6A). We thus performed an unbiased screen of TA proteins to find out GET substrates that can mislocalize to mitochondria and be cleared by Msp1.

In addition to Pex15, there are 48 non-mitochondrial TA proteins encoded by the yeast genome (Appendix Table S1) [36]. We epichromosomally overexpressed all of them in *get3Δ msp1Δ* cells and observed that 34 TA proteins did not localize to mitochondria (Fig EV5A), the expression of six TA proteins was undetectable (Fig EV5B), and eight TA proteins (Frt1, Ysy6, Gos1, Ubc6, Sss1, Far10, Sps2, and Vps64) accumulated on mitochondria (Fig EV5C).

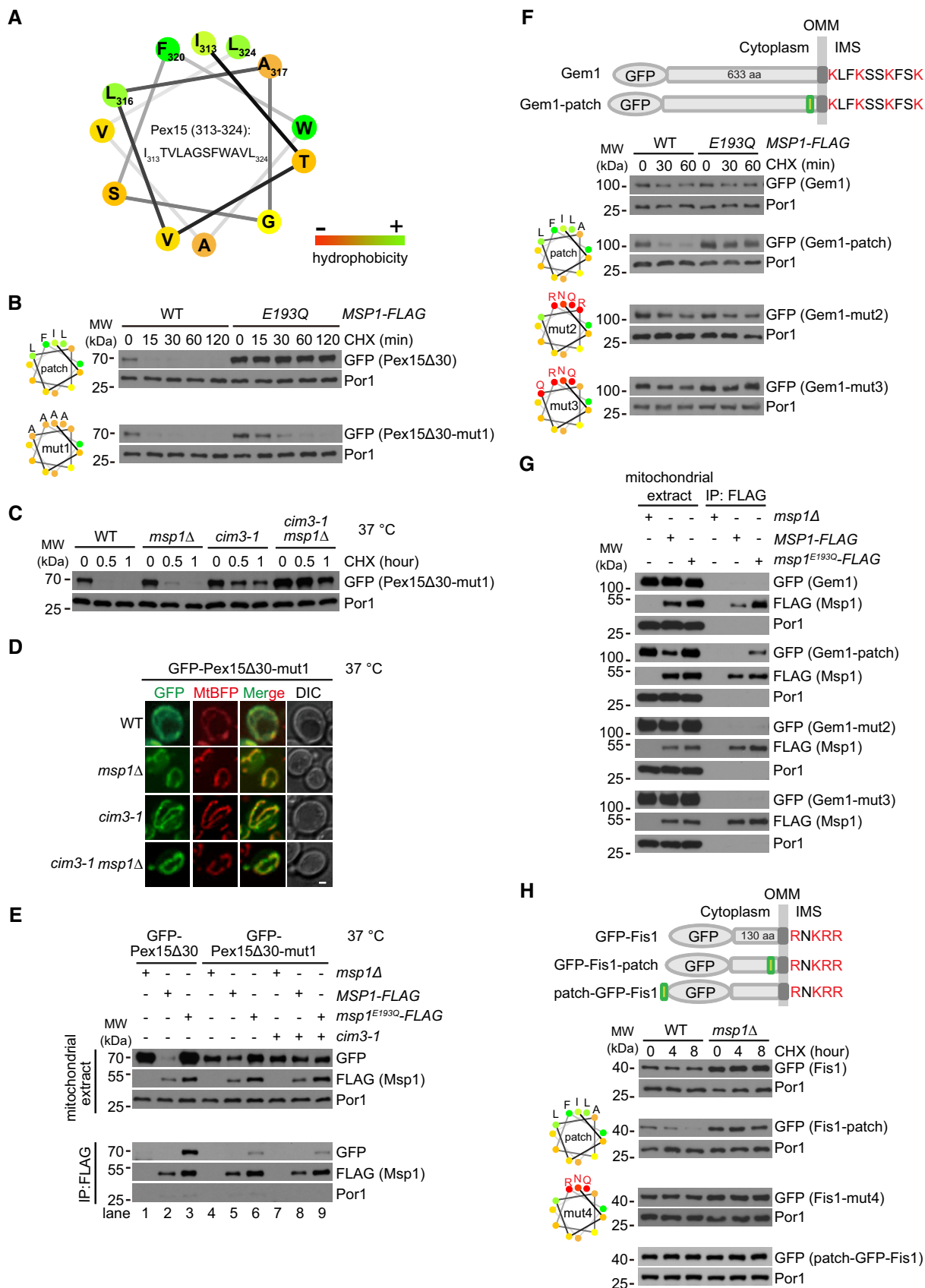


Figure 4.

Figure 4. Patch hydrophobicity of Pex15Δ30 is critical for its interaction with Msp1 and insertion of the patch into mitochondrial TA proteins Fis1 and Gem1 transforms them into Msp1 substrates.

- A Helical wheel plot of the hydrophobic patch of Pex15 (amino acids 313–324). Residues are color-coded according to the hydrophobicity scores.
- B Degradation of GFP-Pex15Δ30 with WT or mutant hydrophobic patch in the indicated strains. Shown on the left are helical wheel plots of WT and mutant (mut1) hydrophobic patches of Pex15. Residue hydrophobicity is color-coded as in (A). The mut1 form carries I313A, L316A, F320A, and L324A mutations.
- C Degradation of GFP-Pex15Δ30-mut1 in the indicated mutants. Cim3-1 is a temperature-sensitive mutant of Cim3. Cells were cultured at 37°C for 1 h to inactivate Cim3 and then treated with CHX.
- D Localization of GFP-Pex15Δ30-mut1 to mitochondria in the indicated strains. Cells were cultured at 37°C for 1 h before imaging. Scale bar represents 1 μm.
- E Interaction of WT and mutant GFP-Pex15Δ30 with Msp1- and Msp1^{E193Q}-FLAG. Cells were cultured at 37°C for 1 h before mitochondria purification. Mitochondrial extracts were subject to anti-FLAG IP and analyzed as in Fig 1D.
- F Insertion of Pex15 hydrophobic patch but not its hydrophilic mutants transforms Gem1 into Msp1 substrate. The patch was inserted between V628 and D629 of Gem1 (before Gem1 OTS) as shown in the upper panel. The mut2 form carries I313N, A317R, F320R, and L324Q mutations. The mut3 form carries I313N, L316Q, F320R, L324Q mutations.
- G Interaction of GFP-Gem1 and its insertion mutants with Msp1- and Msp1^{E193Q}-FLAG. Mitochondrial extracts were subject to anti-FLAG IP and analyzed as in Fig 1D.
- H Insertion of Pex15 hydrophobic patch before Fis1 OTS but not at the N-terminus transforms Fis1 into Msp1 substrate. The insertion was placed between Q125 and K126 of Fis1 (before Fis1 OTS) or at the N-terminus. The mut4 form carries I313N, F320R, L324Q mutations.

Data information: In this figure, GFP-tagged Pex15Δ30, Gem1, Fis1, and their mutants were expressed from a centromeric plasmid under the control of *TEF1* promoter, and Msp1- and Msp1^{E193Q}-FLAG were expressed from the endogenous chromosomal locus.

Tail charge and TM hydrophobicity as indicated by TM GRAVY score have been suggested as important determinants of TA protein sorting [8,30,37]. The TA proteins with mitochondrial mislocalization had medium TM GRAVY score (1.7–2.6) and zero or positive tail charge. But these two parameters are not predictive because many TA proteins in this range did not mislocalize to mitochondria (Fig EV5D).

We continued to analyze the eight TA proteins by chromosomal expression with their endogenous promoters. As shown in Fig 6A, GFP-Frt1 was undetectable in WT, *get3Δ*, and *msp1Δ* cells, but strongly accumulated on mitochondria (pointed by arrows) in about 95% of *get3Δ msp1Δ* cells. GFP-Ysy6 localized to the ER in WT, *get3Δ*, and *msp1Δ* cells, but dually localized to the ER (pointed by arrowheads) and mitochondria (pointed by arrows) in about 95% of *get3Δ msp1Δ* cells, indicating that in *get3Δ* cells, GFP-Ysy6 is partially mistargeted to mitochondria and removed by Msp1. GFP-tagged Gos1 and Ubc6 exhibited very weak mitochondrial localization in a small number of cells (< 5%). GFP-Sss1 did not localize to mitochondria in all the cells examined. GFP-tagged Far10, Sps2, and Vps64 were undetectable. In summary, we identified two TA proteins Frt1 and Ysy6 that prominently mislocalize to mitochondria in *get3Δ* cells and get cleared by Msp1. Most TA proteins did not mislocalize to mitochondria in *get3Δ* cells probably because there are additional complexes to target TA proteins to the ER, such as the SND [38] and the EMC [39] complexes.

Evaluation of Msp1 N-domain critical residues in the removal of GET pathway substrates

Frt1 IMS tail contains three positively charged residues but Ysy6 IMS tail has none (Fig 6B). Like Pex15Δ30, the positively charged IMS tail is critical for the mitochondrial mislocalization of Frt1 (Fig 6C). If Msp1 D12 residue only contributes to interaction with substrates and has no additional roles for Msp1 activity, then the D12T mutation should result in the mitochondrial accumulation of GFP-Frt1 but not GFP-Ysy6 in *get3Δ* cells. Indeed, in *get3Δ msp1^{D12T}* cells, about 50% of cells showed mitochondrial accumulation of GFP-Frt1, and mitochondrial signals of GFP-Ysy6 were not detected (Fig 6D and E).

Hydrophobicity analysis of Frt1 and Ysy6 cytoplasmic domains did not reveal a hydrophobic patch near their TM segments

(Fig 6B). Ysy6 has a short hydrophilic cytoplasmic domain with distributed hydrophobic residues. We then examined whether Msp1 N-domain critical residues, especially hydrophobic ones, are still required for substrate clearance (Fig 6E). L77 and G94 mutations had no or very minor effects on substrate removal. L69, I86, and L96 had a more prominent role in GFP-Frt1 removal. Y72, E73, V81, I93, and G95 were generally required for the removal of both substrates. These results indicate that although a localized hydrophobic patch was not found in Frt1 and Ysy6, Msp1 may still recognize them through hydrophobic interactions in the cytoplasm. Consistent with imaging results, under respiratory growth conditions (SCEG), Msp1 L77A and G94A mutations had no effects on the growth of *get3Δ* cells, D12T, I86A, and L96A mutations partially compromised the growth of *get3Δ* cells, and Y72A, E73A, V81A, I93A, and G95A mutations strongly inhibited the growth of *get3Δ* cells (Fig 6F).

Discussion

Our extensive characterizations of Msp1 and its substrates demonstrate that Msp1 recognizes exposed hydrophobic surfaces of mistargeted TA proteins. An important consequence of protein mislocalization is the loss of their binding partners. This is true for Pex15, which complexes with Pex3 at peroxisome [17], for Frt1, which interacts with Frt2 at the ER [40], and may also apply to the poorly characterized protein Ysy6. Losing binding partners may cause structural deformation and instability to expose hydrophobic surfaces. The crystal structure of Msp1 monomer [21] shows that the critical hydrophobic residues of N-domain for substrate binding are packed against the large AAA-domain to form a closed conformation (Fig 1E). N-domain may exist in a dynamic equilibrium of closed and open conformations to allow Msp1 to sample substrate surfaces and avoid prolonged exposure of its own hydrophobic surfaces. When hydrophobic surfaces of substrates are detected, Msp1 may undergo conformational rearrangements to assemble active hexamers capable of ATP hydrolysis and substrate dislocation (Fig 7).

An unexpected mechanism of substrate recognition by Msp1 is the involvement of a second layer of interaction with substrates

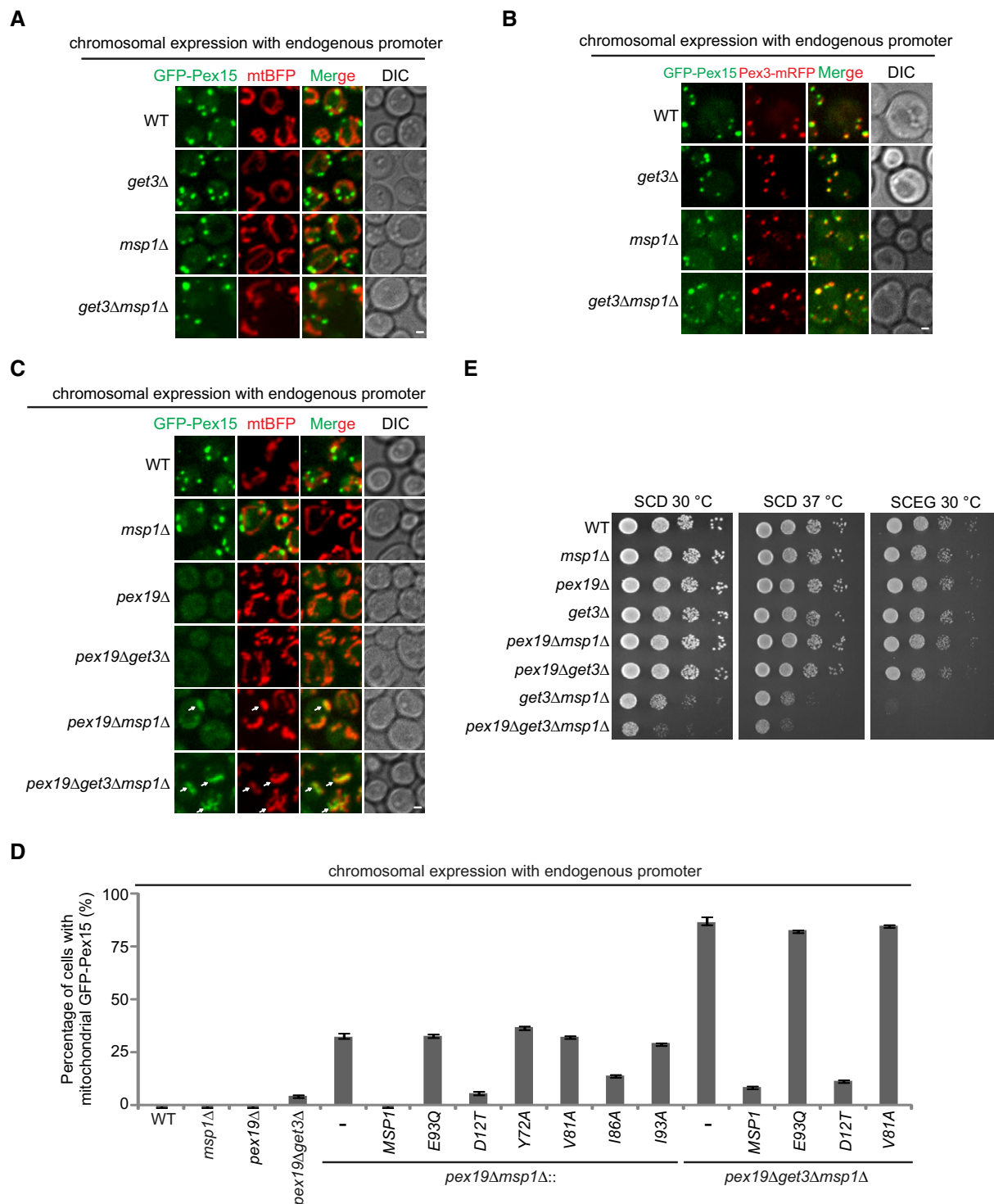


Figure 5. Pex15 is mislocalized to mitochondria and removed by Msp1 in *pex19Δ* cells.

A Chromosomally expressed GFP-Pex15 driven by endogenous promoter did not mislocalize to mitochondria in *GET3* and *MSP1* mutant strains.

B GFP-Pex15 expressed as in (A) localizes to peroxisome in *GET* and *MSP1* mutant strains. Pex3 was chromosomally tagged with mRFP to visualize peroxisomes.

C Localization of GFP-Pex15 expressed as in (A) in the indicated strains. Arrows point to mislocalized GFP-Pex15 on mitochondria.

D The percentage of cells with mitochondrial GFP-Pex15 in the indicated strains. Data values represent means \pm SEM from three independent experiments, with at least 100 cells counted in each experiment.

E The indicated strains were grown in glucose media to log phase and then spotted on SCD or SCEG plates in a 10-fold serial dilution, and then incubated at indicated temperatures for 2–5 days.

Data information: Scale bars in (A–C) represent 1 μ m.

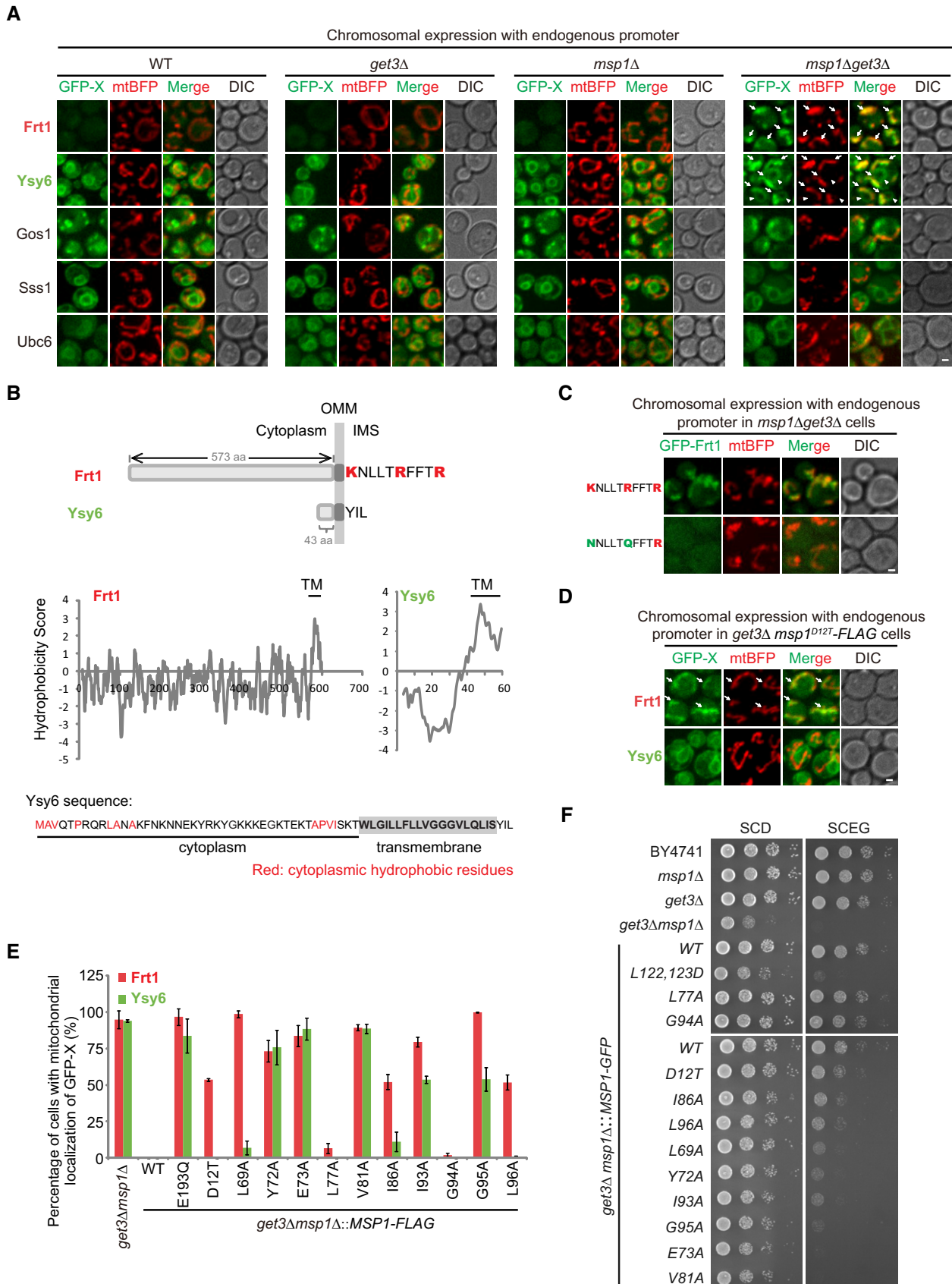
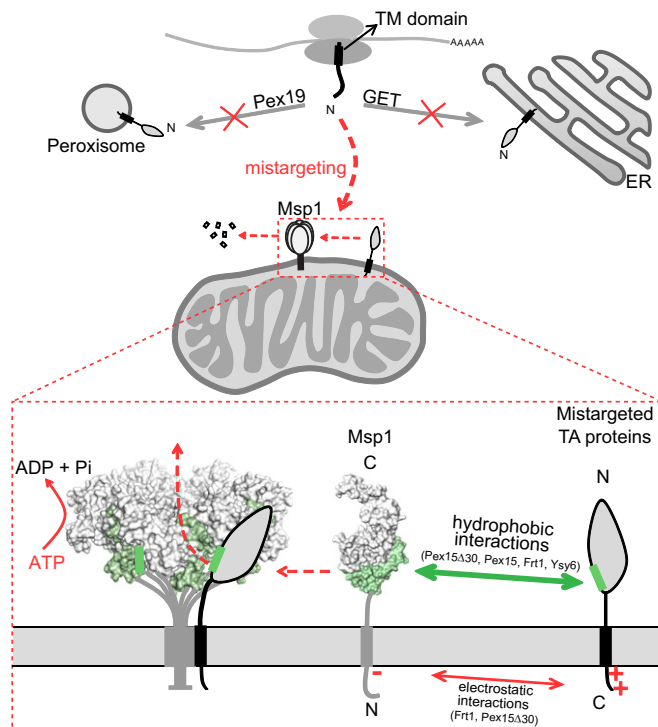


Figure 6.

Figure 6. Identification of TA proteins that are mislocalized to mitochondria and removed by Msp1 in *get3Δ* cells.

- A Localization of GFP-tagged TA proteins in the indicated strains. Arrows point to the mitochondrial GFP-Frt1 and GFP-Ysy6 signals. Arrowheads point to GFP-Ysy6 signals at the ER.
- B Schematic illustration of the IMS tail and sequence hydrophobicity of Frt1 and Ysy6. The amino acid sequence of Ysy6 is shown with the cytoplasmic hydrophobic residues highlighted in red.
- C Localization of GFP-Frt1 with WT or mutant IMS tail in *msp1Δ get3Δ* cells.
- D Localization of GFP-Frt1 and GFP-Ysy6 in *get3Δ msp1^{D12T}-FLAG* mutant cells. Arrows point to mitochondrial GFP-Frt1.
- E The percentage of cells with mitochondrial GFP-Frt1 or GFP-Ysy6 in *get3Δ* cells expressing WT or mutant forms of Msp1-FLAG. Data values represent means \pm SEM from three independent experiments, with at least 50 cells counted in each experiment.
- F The indicated strains were grown in glucose media to log phase and then spotted on SCD or SCEG plates in a 10-fold serial dilution, and then incubated at 30°C for 2–5 days.

Data information: In this figure, a gene cassette expressing GFP-tagged TA protein under the control of endogenous promoter was integrated at the *his3* locus, and WT or mutant forms of Msp1-FLAG were expressed from the endogenous chromosomal locus. Scale bars in (A, C, and D) represent 1 μ m.

**Figure 7. A working model for Msp1-mediated clearance of mislocalized TA proteins.**

Newly expressed TA proteins are targeted to peroxisome and the ER by the Pex19 and GET pathways, respectively. Disrupting these pathways mistargets TA proteins to mitochondria. Mistargeted TA proteins expose hydrophobic surfaces in the cytoplasm and are recognized by Msp1 N-domain hydrophobic residues. The interaction is further facilitated by IMS electrostatic interactions when substrates contain positively charged IMS tails. Substrate-engaged Msp1 assembles into hexamer to dislocate substrates through ATP hydrolysis.

Pex15Δ30 and Frt1 at the IMS side, very likely through electrostatic interactions between positively charged residues of substrates and the negatively charged D12 residue of Msp1 (Fig 7). Positively charged residues in IMS tail are critical for the targeting of mitochondrial and peroxisomal TA proteins [8,29], and also required for mistargeting of Pex15Δ30 and Frt1 to mitochondria (Figs EV3A and 6C). Recognizing this property enables Msp1 to survey a large number of mitochondrial and peroxisomal TA proteins. When dual interactions in the IMS and cytoplasmic domains occur, the affinity

between Msp1 and substrates will be substantially enhanced to enable efficient substrate removal and thus enable Msp1 to safeguard mitochondrial function at its physiological expression level, as suggested by the suboptimal growth of *get3Δ msp1^{D12T}* cells (Fig 6F).

These results together highlight a crucial role of Msp1 N-domain in substrate recognition, a feature of the meiotic clade of AAA-ATPases [20]. Considering that Msp1 recognizes misfolded domains with exposed hydrophobic surfaces, it may have a more general role in the quality control of OMM and peroxisomal proteins beyond mistargeted TA proteins. Consistent with this, Msp1 was recently found to remove mitochondrial precursor proteins clogged in the TOM import channel [22].

Materials and Methods

Culture media

Media used in this study included standard YP and synthetic minimal media supplemented with 2% glucose (D), 2% lactate(L), 2% galactose (Gal), or 3% ethanol and glycerol (EG). The synthetic media contained either complete supplements or the appropriate amino acid dropout mixture. ClonNAT (100 μ g/l, WERNER BioAgents) was added to media for plasmid maintenance as needed. Yeast strains were grown at 30°C if not otherwise indicated.

Yeast strains and plasmids

The yeast strains used in this study are listed in Appendix Table S2. Strain transformation was performed using the lithium acetate method, selected on appropriate media, and confirmed by PCR and gene expression as needed [41–43]. The strains expressing Msp1 variants from the endogenous loci were generated by PCR-based homologous recombination to replace the original selection cassette in *msp1Δ* strain with cassettes containing sequences encoding WT or mutant forms of *MSP1* and a different selection marker. The *msp1Δget3Δ* strains epichromosomally expressing Msp1 variants were generated using the systematic genetic analysis (SGA) technique [44]: (i) *msp1Δ* strain (in BY4741 background) was mated with *get3Δ* strain (in Y7092 background). (ii) The resulting diploid strain was transformed with an empty vector or a centromeric plasmid expressing WT or mutant forms of Msp1 under the control of its endogenous promoter. (iii) The resulting strain was cultured in

sporulation media and then subject to a series of selection processes for the isolation of the desired haploid strains.

The plasmids used in this study (Appendix Table S3) were generated using the Gibson-based assembly method [45]. Mutations were created by Quick Change site-directed mutagenesis (Stratagene).

Antibodies and chemicals

The following antibodies were from Sigma: G6PDH produced in rabbit (A9521), HA-peroxidase (H6533), and FLAG M2 produced in mouse (F1804). The antibody for Por1 produced in mouse (459500) was from Life Technologies. The antibody for GFP produced in mouse (11814460001) was from Roche. A synthetic peptide (amino acid residues CTLDAYERTILSSIV of Msp1) was used to generate Msp1 antibody.

Yeast extract, peptone, and yeast nitrogen base without amino acids were from BD Biosciences. Yeast complete supplement mixture was from MP Biomedicals. Yeast amino acid dropout supplements were from Clontech. Cycloheximide (used at 50 µg/ml) was from Amresco. Benzoyl-phenylalanine (BPA) was from Bachem. Other chemicals or reagents were from Sigma if not otherwise indicated.

Yeast whole cell extract preparation and thermostability measurement

Cell pellets were resuspended in 300 µl yeast lysis buffer (50 mM NaCl, 50 mM NaF, 100 mM Tris-HCl (pH 7.5), 1 mM EDTA, 1 mM EGTA, 1% Triton X-100, 10% glycerol, 14 mM 2-mercaptoethanol, 2 mM PMSF, 5 µM pepstatin A, 10 µM Leupeptin). After adding ~80 µl of glass beads, cells were lysed via three rounds of bead-beating (40 s beating followed by 1 min of cooling on ice).

Cell extracts were divided into equal volume (50 µl) and heated at the indicated temperatures for 3 min on a PCR machine followed by cooling down to 4°C on ice. Heated cell lysates were centrifuged at 18,407 g for 10 min at 4°C to collect supernatants. Equal volume of supernatants was analyzed by Western blot. Band intensity was measured by ImageJ software.

Purification of recombinant proteins and limited trypsin digestion

Msp1 (33–345) was amplified by PCR from plasmid and subcloned into a pET28a derivative encoding an N-terminal 6xHis-Smt3 tag. Site-specific mutagenesis was performed by Quick Change PCR. All plasmids were confirmed by DNA sequencing.

Plasmids were transformed into Rosetta (DE3). Cells were grown at 37°C until an OD₆₀₀ of 0.6–1.0. Cultures were induced with 1 mM IPTG (Sigma) and grown at 18°C for 16–18 h. Cells were harvested by centrifugation, and resuspended in lysis buffer (20 mM Tris-HCl pH 8.0, 500 mM NaCl, 1 mM PMSF, 10 mM imidazole), and lysed by sonication. The supernatant was isolated by centrifugation for 1 h at 4°C at 38,759 g. The supernatant was filtered with 0.22-µm filter and purified by Ni-NAT column. Ni-NTA resin was washed with 10 column volumes (CV) of lysis buffer and 10 CV of wash buffer (lysis buffer with 30 mM imidazole), then eluted with lysis buffer containing 250 mM imidazole. After Ni-NTA purification, protein concentrations were determined by Bradford assay. Recombinant proteins were treated with 1/100

SUMO Protease 1 (Ulp1) for 16 h at 4°C to cleave off the 6xHis-Smt3 tag, and reloaded to Ni-NAT column to remove the tag. Recombinant proteins were digested with 1/500 (by concentration) trypsin at 37°C for the indicated times and then subjected to SDS-PAGE and Coomassie Blue staining.

Isolation of the mitochondria-enriched fraction and immunoprecipitation

Mitochondria were isolated following a previously described method [46], with some modifications. Briefly, about 200 ml of cells grown in synthetic glucose media to late log phase (OD ~ 3) was collected. Cells were washed once with water and incubated in TD buffer [10 mM DTT, 100 mM Tris-SO₄ (pH 9.4)] for 15 min at 30°C. Cells were then washed once with SP buffer [1.2 M sorbitol, 20 mM potassium phosphate (pH 7.4)] and treated with Zymolyase 20T/100T (MP Biomedicals) for 40 min at 30°C to generate spheroplasts. After two times of washes with SP buffer, the spheroplasts were resuspended in SHE buffer [0.6 M sorbitol, 20 mM HEPES-KOH (pH 7.4), 1 mM EGTA (pH 8), 2 mM MgCl₂] supplemented with protease inhibitors and homogenized by a French press (EmulsiFlex-C3, AVESTIN Inc.) at pressures in the range of 1,000 to 1,500 psi. The mitochondria-enriched fraction was obtained by differential centrifugation, flash frozen by liquid nitrogen, and stored at –80°C until use.

Crude mitochondria were solubilized with 1% digitonin buffer [50 mM HEPES-KOH (pH 7.4), 50 mM KOAc, 2 mM Mg(OAc)₂, 1 mM CaCl₂, 200 mM sorbitol, 1 mM NaF, 1% (w/v) digitonin] supplemented with 1 mM DTT, 2 mM ATP, and protease inhibitors for 45–60 min at 4°C. The lysates were cleared by centrifugation at 17,000 g for 10 min at 4°C. The supernatant was then mixed with anti-FLAG agarose beads (Sigma) and incubated at 4°C for 5–6 h. The agarose beads were then washed five times with 0.1% digitonin buffer and eluted overnight with FLAG peptide (ChinaPeptides Co. Ltd.) at 4°C.

Site-specific *in vivo* photo-crosslinking and immunoprecipitation

Experiments were performed following a previously described method [23] with specific modifications as follows. For GFP-3xHA-Pex15Δ30-BPA, strains in W303 background were transformed with two 2-µ plasmids: One expresses GFP-3xHA-Pex15Δ30 with an amber (TAG) codon at a specific site under the control of the repressible *GAL1* promoter; and the other one expresses an amber suppressor tRNA and a modified aminoacyl-tRNA synthetase that specifically charges the amber suppressor tRNA with the photo-reactive unnatural amino acid BPA. For Msp1-BPA, a gene cassette expressing Msp1 with TAG codon under the control of *GAL1* promoter was integrated into *his3* locus. The resulting strain was transformed with the same plasmid to express the tRNA and tRNA ligase. Strains were grown in selective glucose media to late log phase and then switched to BPA (0.2 mM)-containing selective media supplemented with 2% lactate and 0.05% galactose for Msp1-BPA or 2% galactose for Pex15Δ30-BPA for 16–18 h. About 80 OD₆₀₀ units of cells in late log phase were subject to UV irradiation for 15 min. To prepare whole cell extracts, cells were resuspended in 0.1 M NaOH and incubated at room temperature for 5–10 min. Cell pellets were then resuspended in SDS buffer [50 mM Tris-HCl (pH 7.5), 150 mM NaCl, 2% (w/v) SDS, 4% (v/v) BME]

and boiled at 98°C for 10 min. The lysates were cleared by centrifugation at 17,000 g for 10 min. The supernatant was then diluted with 15 volumes of Triton buffer (50 mM Tris-HCl (pH 7.5), 150 mM NaCl, 1% (v/v) Triton), mixed with anti-FLAG agarose beads, and incubated at 4°C for 5–6 h. The agarose beads were then washed four times with Triton buffer and eluted overnight with FLAG peptide at 4°C.

Microscopy

Yeast cells were grown in synthetic glucose media to log phase, concentrated, and immobilized on microscope slides. Fluorescent images were captured at 25°C using a 100× objective (CFI Plan Apochromat Lambda; NA 1.45; Nikon) with immersion oil (type NF) on an inverted fluorescence microscope (Eclipse Ti-E; Nikon) with a spinning-disk confocal scanner unit (UltraView; PerkinElmer) with 488 [emission filter 525 (W50)] and 405 [emission filter 445 (W60) and 615 (W70)] lasers. Z-stack images with 0.5 μm increments were acquired with Volocity software (PerkinElmer) and processed with Volocity and ImageJ software.

Sequence, structure, and bioinformatics analysis

Sequence alignment was performed using ClustalW and processed by GeneDoc software. The structure of monomeric or hexameric form of Msp1 was analyzed and processed using PyMOL. The GRAVY (Grand Average of Hydropathicity) values of TM domains and the hydrophobicity plot of Pex15Δ30 were calculated using the ProtParam and ProtScale server, respectively, from ExPASy. The charges of TM domain flanking sequences were calculated using the Protein Calculator v3.4 (<http://protcalc.sourceforge.net>). The helical wheel plots were generated using the helical wheel projections server (<http://rzlab.ucr.edu/scripts/wheel/wheel.cgi>). Protein topology model was generated using the Protter server (<http://wlab.thz.ch/protter/#>).

Expanded View for this article is available online.

Acknowledgements

We thank Dr. Charlie Boone (University of Toronto, Canada) for providing the Y7092 strain. The research is supported by National Natural Science Foundation of China (Grant No. 31871346), the National Basic Research Program of China 973 (program 2012CB837503), and Beijing Municipal Science and Technology Commission. X.W. is supported by Beijing Postdoctoral Research Foundation and China Postdoctoral Science Foundation.

Author contributions

HJ and XW conceived the project, supervised the study, and wrote the manuscript. LL generated substrates and their mutations and analyzed their localization and turnover. LL performed thermostability analysis of Msp1 and its mutants and generated recombinant proteins and performed limited trypsin digestion. JZ generated Msp1 mutants, analyzed their effects on substrate degradation, and performed immunoprecipitation and blue-native gel experiments. JZ and LL performed the *in vivo* site-specific photo-crosslinking experiments.

Conflict of interest

The authors declare that they have no conflict of interest.

References

- Gerdes F, Tatsuta T, Langer T (2012) Mitochondrial AAA proteases—towards a molecular understanding of membrane-bound proteolytic machines. *Biochim Biophys Acta* 1823: 49–55
- Baker MJ, Tatsuta T, Langer T (2011) Quality control of mitochondrial proteostasis. *Cold Spring Harb Perspect Biol* 3: a007559
- Karbowski M, Youle RJ (2011) Regulating mitochondrial outer membrane proteins by ubiquitination and proteasomal degradation. *Curr Opin Cell Biol* 23: 476–482
- Bragoszewski P, Turek M, Chacinska A (2017) Control of mitochondrial biogenesis and function by the ubiquitin-proteasome system. *Open Biol* 7: 170007
- Wu X, Li L, Jiang H (2016) Doa1 targets ubiquitinated substrates for mitochondria-associated degradation. *J Cell Biol* 213: 49–63
- Chen YC, Umanah GK, Dephoure N, Andrabi SA, Gygi SP, Dawson TM, Dawson VL, Rutter J (2014) Msp1/ATAD1 maintains mitochondrial function by facilitating the degradation of mislocalized tail-anchored proteins. *EMBO J* 33: 1548–1564
- Okreglak V, Walter P (2014) The conserved AAA-ATPase Msp1 confers organelle specificity to tail-anchored proteins. *Proc Natl Acad Sci USA* 111: 8019–8024
- Borgese N, Colombo S, Pedrazzini E (2003) The tale of tail-anchored proteins: coming from the cytosol and looking for a membrane. *J Cell Biol* 161: 1013–1019
- Hegde RS, Keenan RJ (2011) Tail-anchored membrane protein insertion into the endoplasmic reticulum. *Nat Rev Mol Cell Biol* 12: 787–798
- Denic V, Dotsch V, Sinning I (2013) Endoplasmic reticulum targeting and insertion of tail-anchored membrane proteins by the GET pathway. *Cold Spring Harb Perspect Biol* 5: a013334
- Schuldiner M, Metz J, Schmid V, Denic V, Rakwalska M, Schmitt HD, Schwappach B, Weissman JS (2008) The GET complex mediates insertion of tail-anchored proteins into the ER membrane. *Cell* 134: 634–645
- Mozdy AD, McCaffery JM, Shaw JM (2000) Dnm1p GTPase-mediated mitochondrial fission is a multi-step process requiring the novel integral membrane component Fis1p. *J Cell Biol* 151: 367–380
- Kornmann B, Osman C, Walter P (2011) The conserved GTPase Gem1 regulates endoplasmic reticulum-mitochondria connections. *Proc Natl Acad Sci USA* 108: 14151–14156
- Wiedemann N, Pfanner N (2017) Mitochondrial machineries for protein import and assembly. *Annu Rev Biochem* 86: 685–714
- Kemper C, Habib SJ, Engl G, Heckmeyer P, Dimmer KS, Rapaport D (2008) Integration of tail-anchored proteins into the mitochondrial outer membrane does not require any known import components. *J Cell Sci* 121: 1990–1998
- Setoguchi K, Otera H, Mihara K (2006) Cytosolic factor- and TOM-independent import of C-tail-anchored mitochondrial outer membrane proteins. *EMBO J* 25: 5635–5647
- Weir NR, Kamber RA, Martenson JS, Denic V (2017) The AAA protein Msp1 mediates clearance of excess tail-anchored proteins from the peroxisomal membrane. *Elife* 6: e28507
- Piard J, Umanah GKE, Harms FL, Abalde-Atristain L, Amram D, Chang M, Chen R, Alawi M, Salpietro V, Rees MI et al (2018) A homozygous ATAD1 mutation impairs postsynaptic AMPA receptor trafficking and causes a lethal encephalopathy. *Brain* 141: 651–661
- Frickey T, Lupas AN (2004) Phylogenetic analysis of AAA proteins. *J Struct Biol* 146: 2–10

20. Monroe N, Hill CP (2016) Meiotic clade AAA ATPases: protein polymer disassembly machines. *J Mol Biol* 428: 1897–1911
21. Wohlever ML, Mateja A, McGilvray PT, Day KJ, Keenan RJ (2017) Msp1 is a membrane protein dislocase for tail-anchored proteins. *Mol Cell* 67: 194–202 e196
22. Weidberg H, Amon A (2018) MitoCPR-A surveillance pathway that protects mitochondria in response to protein import stress. *Science* 360: eaan4146
23. Shiota T, Nishikawa S, Endo T (2013) Analyses of protein-protein interactions by *in vivo* photocrosslinking in budding yeast. *Methods Mol Biol* 1033: 207–217
24. Chin JW, Cropp TA, Anderson JC, Mukherji M, Zhang Z, Schultz PG (2003) An expanded eukaryotic genetic code. *Science* 301: 964–967
25. Shiota T, Imai K, Qiu J, Hewitt VL, Tan K, Shen HH, Sakiyama N, Fukasawa Y, Hayat S, Kamiya M et al (2015) Molecular architecture of the active mitochondrial protein gate. *Science* 349: 1544–1548
26. Shiota T, Mabuchi H, Tanaka-Yamano S, Yamano K, Endo T (2011) *In vivo* protein-interaction mapping of a mitochondrial translocator protein Tom22 at work. *Proc Natl Acad Sci USA* 108: 15179–15183
27. Wu X, Li L, Jiang H (2018) Mitochondrial inner-membrane protease Yme1 degrades outer-membrane proteins Tom22 and Om45. *J Cell Biol* 217: 139–149
28. Martin A, Baker TA, Sauer RT (2008) Diverse pore loops of the AAA+ ClpX machine mediate unassisted and adaptor-dependent recognition of ssrA-tagged substrates. *Mol Cell* 29: 441–450
29. Rapaport D (2003) Finding the right organelle. Targeting signals in mitochondrial outer-membrane proteins. *EMBO Rep* 4: 948–952
30. Costello JL, Castro IG, Camões F, Schrader TA, McNeill D, Yang J, Giannopoulou EA, Gomes S, Pogenberg V, Bonekamp NA et al (2017) Predicting the targeting of tail-anchored proteins to subcellular compartments in mammalian cells. *J Cell Sci* 130: 1675–1687
31. Rottensteiner H, Kramer A, Lorenzen S, Stein K, Landgraf C, Volkmer-Engert R, Erdmann R (2004) Peroxisomal membrane proteins contain common Pex19p-binding sites that are an integral part of their targeting signals. *Mol Biol Cell* 15: 3406–3417
32. Hettema EH, Girzalsky W, van Den Berg M, Erdmann R, Distel B (2000) *Saccharomyces cerevisiae* pex3p and pex19p are required for proper localization and stability of peroxisomal membrane proteins. *EMBO J* 19: 223–233
33. Jones JM, Morrell JC, Gould SJ (2004) PEX19 is a predominantly cytosolic chaperone and import receptor for class 1 peroxisomal membrane proteins. *J Cell Biol* 164: 57–67
34. Halbach A, Landgraf C, Lorenzen S, Rosenkranz K, Volkmer-Engert R, Erdmann R, Rottensteiner H (2006) Targeting of the tail-anchored peroxisomal membrane proteins PEX26 and PEX15 occurs through C-terminal PEX19-binding sites. *J Cell Sci* 119: 2508–2517
35. Yagita Y, Hiromasa T, Fujiki Y (2013) Tail-anchored PEX26 targets peroxisomes via a PEX19-dependent and TRC40-independent class I pathway. *J Cell Biol* 200: 651–666
36. Burri L, Lithgow T (2004) A complete set of SNAREs in yeast. *Traffic* 5: 45–52
37. Rao M, Okreglak V, Chio US, Cho H, Walter P, Shan SO (2016) Multiple selection filters ensure accurate tail-anchored membrane protein targeting. *Elife* 5: e21301
38. Aviram N, Ast T, Costa EA, Arakel EC, Chuartzman SG, Jan CH, Haßdenteufel S, Dudek J, Jung M, Schorr S et al (2016) The SND proteins constitute an alternative targeting route to the endoplasmic reticulum. *Nature* 540: 134–138
39. Guna A, Volkmar N, Christianson JC, Hegde RS (2018) The ER membrane protein complex is a transmembrane domain insertase. *Science* 359: 470–473
40. Heath VL, Shaw SL, Roy S, Cyert MS (2004) Hph1p and Hph2p, novel components of calcineurin-mediated stress responses in *Saccharomyces cerevisiae*. *Eukaryot Cell* 3: 695–704
41. Longtine MS, McKenzie III A, Demarini DJ, Shah NG, Wach A, Brachet A, Philippsen P, Pringle JR (1998) Additional modules for versatile and economical PCR-based gene deletion and modification in *Saccharomyces cerevisiae*. *Yeast* 14: 953–961
42. Voth WP, Richards JD, Shaw JM, Stillman DJ (2001) Yeast vectors for integration at the HO locus. *Nucleic Acids Res* 29: E59–9
43. Janke C, Magiera MM, Rathfelder N, Taxis C, Reber S, Maekawa H, Moreno-Borchart A, Doenges G, Schwob E, Schiebel E et al (2004) A versatile toolbox for PCR-based tagging of yeast genes: new fluorescent proteins, more markers and promoter substitution cassettes. *Yeast* 21: 947–962
44. Tong AH, Boone C (2006) Synthetic genetic array analysis in *Saccharomyces cerevisiae*. *Methods Mol Biol* 313: 171–192
45. Gibson DG, Young L, Chuang RY, Venter JC, Hutchison III CA, Smith HO (2009) Enzymatic assembly of DNA molecules up to several hundred kilobases. *Nat Methods* 6: 343–345
46. Diekert K, de Kroon AI, Kispal G, Lill R (2001) Isolation and subfractionation of mitochondria from the yeast *Saccharomyces cerevisiae*. *Methods Cell Biol* 65: 37–51